180
8/28/79

Ag. 3066

ORNL/TM-6940

MASTER

Characterization of SiC Coatings on HTGR Fuel Particles: Preliminary Report

R. J. Lauf
D. N. Braski
V. J. Tennery

OAK RIDGE NATIONAL LABORATORY
OPERATED BY UNION CARBIDE CORPORATION · FOR THE DEPARTMENT OF ENERGY

DISCLAIMER

Printed in the United States of America. Available from
National Technical Information Service
U.S. Department of Commerce
5285 Port Royal Road, Springfield, Virginia 22161
Price: Printed Copy $4.50 ; Microfiche $3.00

ORNL/TM-6940
Distribution
Category UC-77

Contract No. W-7405-eng-26

METALS AND CERAMICS DIVISION

HTGR BASE TECHNOLOGY PROGRAM

Fueled Graphite Development (189a 01330)

CHARACTERIZATION OF SiC COATINGS ON HTGR FUEL PARTICLES: PRELIMINARY REPORT

R. J. Lauf
D. N. Braski
V. J. Tennery

Date Published: August 1979

NOTICE This document contains information of a preliminary nature. It is subject to revision or correction and therefore does not represent a final report.

OAK RIDGE NATIONAL LABORATORY
Oak Ridge, Tennessee 37830
operated by
UNION CARBIDE CORPORATION
for the
DEPARTMENT OF ENERGY

THIS PAGE

WAS INTENTIONALLY

LEFT BLANK

CONTENTS

CHARACTERIZATION OF SiC COATINGS ON HTGR FUEL PARTICLES: PRELIMINARY REPORT

R. J. Lauf
D. N. Braski
V. J. Tennery

ABSTRACT

Fuel particles for the HTGR contain a layer of pyrolytic silicon carbide to act as a pressure vessel and fission product barrier. The SiC is deposited by the thermal decomposition of methyltrichlorosilane (CH_3SiCl_3 or MTS) in an excess of hydrogen. Coatings deposited at temperatures from 1500 to 1700°C and coating rates of 0.4 to 1.2 μm/min have been studied by optical microscopy, x-ray diffraction, electron microscopy, and density measurements. Transmission electron microscopy (TEM) has shown the microstructural features to be extremely complex and much finer than the ability of optical microscopy to resolve. X-ray diffraction has detected traces of α-SiC in some coatings, and those conditions of deposition temperature and coating rate that give rise to this phase have been determined. Lattice fringe images of 1.5 nm spacing indicate that the α-SiC observed in TEM is of the 6H polytype. Previously, the coatings were assumed to be all cubic β-SiC. Optical microscopy has indicated that the SiC coatings are optically anisotropic. This result is unexpected in a cubic material and is not completely understood at this time. Coating density varied with deposition temperature and coating rate, in agreement with earlier work.

INTRODUCTION

The fuel system for the High-Temperature Gas-Cooled Reactor (HTGR) consists of fuel microspheres coated with layers of pyrolytic carbon (PyC) and silicon carbide (SiC), as shown in Fig. 1. The low-density buffer layer of PyC provides void volume within the fuel particle for fission gas retention. The inner low-temperature isotropic (ILTI) PyC coating provides mechanical strength to resist the stresses generated by the fission gas pressure of several hundred times atmospheric developed during fuel service. It also provides a containment barrier to

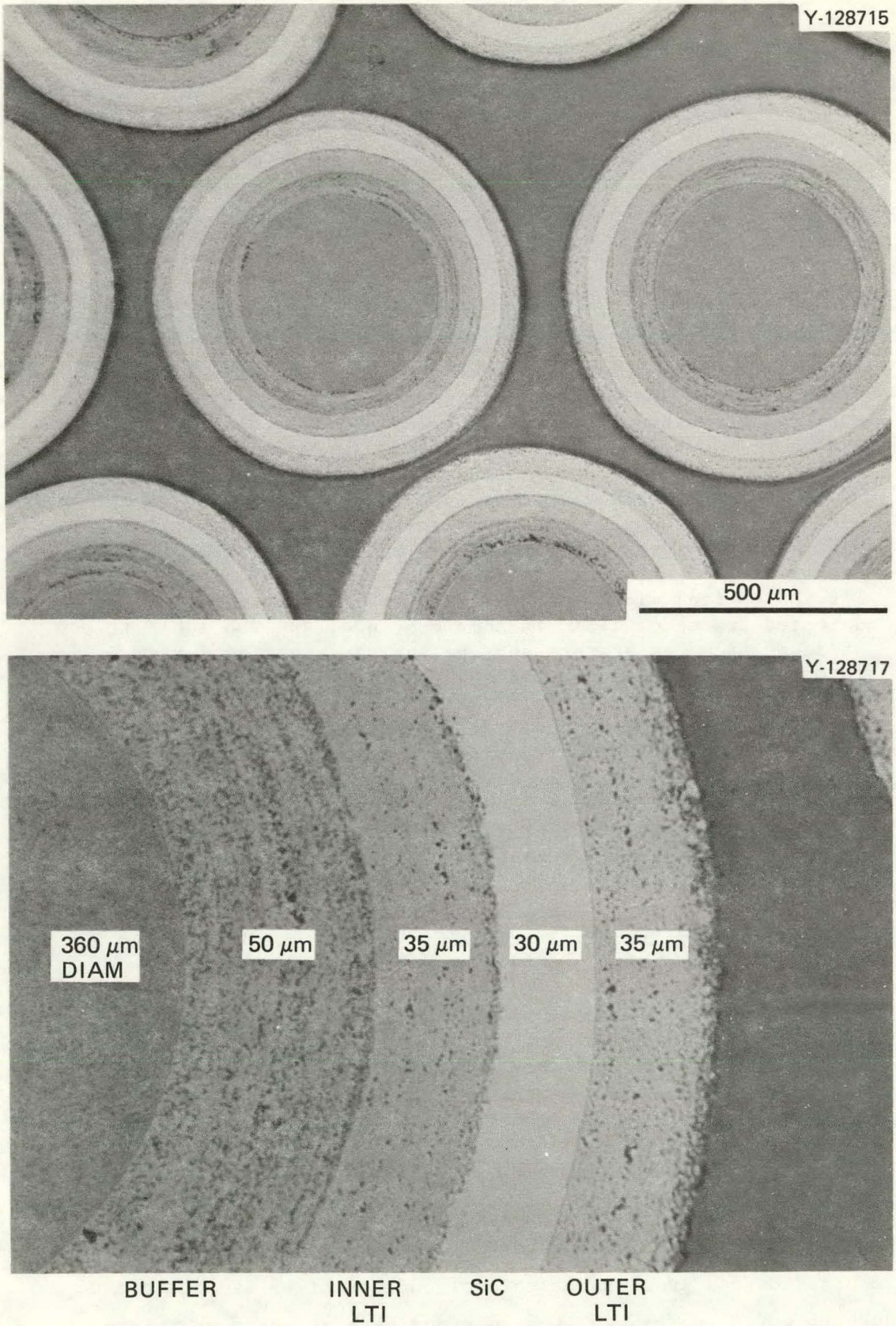

Fig. 1. Coated HTGR Fuel Particles.

some of the fission products that are produced within the kernel and move relatively easily through the buffer coating. The SiC coating or layer also serves as the wall of a micro pressure vessel and more importantly plays the role of a barrier to transport of fission products such as strontium, cesium, barium, and certain rare earths, which are the dominant solid fission products from the fission of ^{235}U under standard conditions. Until 1977, it was anticipated that early HTGRs would be fueled with fuel kernels of relatively high ^{235}U enrichment. The outer LTI PyC coating on the fuel particle illustrated in Fig. 1 mechanically protects the SiC coating during the fabrication of fuel particles into a carbon matrix for subsequent placement into the graphite blocks from which the core of the HTGR is constructed.

Since 1977, the use of reactor fuel systems requiring high enrichments of any fissile species has been undergoing critical assessment because of concerns about the possibility of highly enriched fissile material being diverted from a power reactor fuel cycle and used for the construction of nuclear weapons. This assessment as applied to the HTGR has resulted in an analysis of the proposition of operating the HTGR with so-called low-enriched (LEU) or medium-enriched (MEU) uranium-based fuels. Results available indicate that such fuels can be neutronically viable in HTGRs. From a fuel system operation viewpoint, use of MEU or LEU fuels poses a problem in the sense that the fission product spectra from these fuels are significantly different from that from an HEU fuel. Specifically, the fission products silver and palladium have significantly higher yields in LEU or MEU fuels, and these elements are known to be particularly aggressive to SiC under the conditions operative in an HTGR fuel particle. They also diffuse rapidly through dense PyC at the temperatures of interest. The SiC coatings in fuel particles for MEU or LEU systems must provide most of the containment of these species within the fuel particle.

It is therefore of great importance to MEU or LEU fueled HTGRs that the quantitative characteristics of the SiC coatings on fuel particles be understood, their control be demonstrated, and the coating characteristics necessary to minimize silver and palladium interaction be

identified. The SiC is deposited on the microspheres in a fluidized-bed reaction chamber by the thermal decomposition of methyltrichlorosilane (CH_3SiCl_3 or MTS) in an excess of hydrogen. Previous studies[1,2] have shown a simple relation between the SiC deposition parameters (temperature, coating rate, etc.) and the resulting density. Although the density correlates reasonably well with measured mechanical strength, available data indicate that density alone is inadequate to characterize the SiC as to its ability to resist reaction or diffusion of silver of palladium under HTGR operating conditions. Previous work showed that the microstructural features of high-density SiC coatings on HTGR fuel particles are extremely small, with many of them being smaller than the resolution available with oil immersion objectives on an optical microscope. The purpose of this report is to present a preliminary characterization of the microstructures of the SiC coatings on a very fine scale to produce for this material a data base that can later be used to assist in understanding the irradiation behavior and fission product retention properties of the SiC. This report contains the first results of applying high-resolution electron microscopic techniques to SiC coatings on fuel particles. In addition, more standard data including density, x-ray diffraction, and optical microscopy are also presented. Results provided here are a preliminary part of those being systematically developed for a series of SiC coatings deposited on fuel particles containing silver and palladium as simulated fission products. Analyses of these coatings after long-term thermal gradient testing of the particles will later be used to identify how the silver and palladium interact with the SiC on a microscopic scale.

SiC COATING PREPARATION AND CHARACTERIZATION METHODS

SiC Deposition

Fluidized-Bed Coating System

Particles used in this study were coated with SiC in a fluidized-bed reactor. This device consists of a graphite furnace tube and heating element, gas flow controls, a methyltrichlorosilane (MTS) vapor source, and a scrubber for by-product gases. Because of the small batch sizes used in this study, a 25-mm-ID furnace tube was used. This tube is illustrated in Fig. 2.

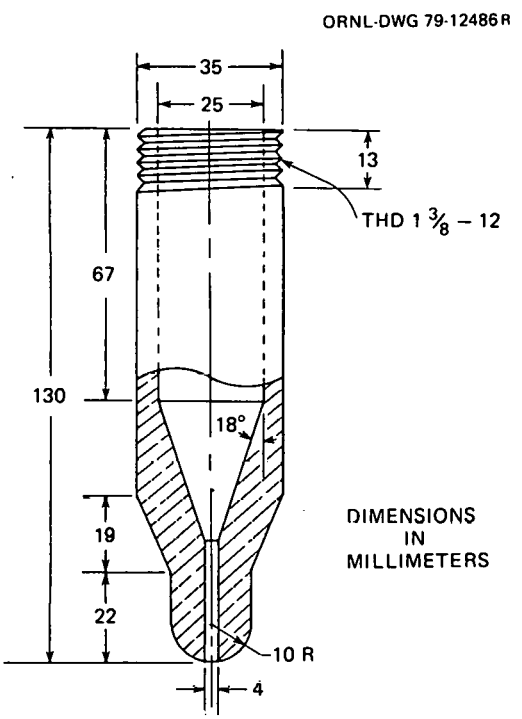

Fig. 2. Graphite Coating Tube.

To provide MTS vapor at controlled rates, a Tylan Source II* controller was used. This instrument measures the MTS vapor

*Tylan Corp., Torrance, Calif.

concentration in the carrier gas stream and continuously adjusts the carrier flow rate to maintain a preset MTS delivery rate. The mixture of hydrogen and MTS from the controller was further diluted with additional "bypass" hydrogen before injection into the orifice of the coating tube. The excess hydrogen served the dual purposes of fluidizing the particle bed and aiding in the decomposition of the MTS.

Flow rates of carrier and bypass hydrogen were measured with rotameters, which had been calibrated with an American Meter Company wet-test meter. The accuracy of the wet-test meter was found to be approximately ±1% by comparison with a volumetor.

The temperature of the fluidized bed was measured with an optical pyrometer sighted through a silica glass window onto the coating tube at a point approximately 50 mm above the apex of the cone. The materials and configuration were such that blackbody conditions were closely approximated. Because of absorption by the silica window, the pyrometer reading was approximately 30°C lower than the bed temperature as measured by a thermocouple.

The by-products of MTS decomposition include hydrogen chloride vapor and various halocarbons.[3,4] These were removed from the off-gas stream by a water scrubber.

Deposition Parameters Investigated

Previous investigations[1,2] showed that silicon carbide of high density can be deposited at temperatures of 1450 to 1700°C and coating rates up to at least 0.5 μm/min. The present study included four temperatures: 1500, 1550, 1650, and 1700°C. Three ranges of coating rates were examined: 0.2 to 0.4, 0.5 to 0.7, and 1.0 to 1.5 μm/min. The experimental matrix of deposition parameters investigated is summarized in Table 1. From each matrix element, coating specimens will be studied by several methods. Those that have been completed for this preliminary study are noted in Table 1. In some cases, the observations were supplemented by study of specimens coated in previous investigations.

Table 1. Experimental Coating Parameters Investigated

Coating Rate (μm/min)	Observation[a] for Each Deposition Temperature in °C			
	1500	1550	1650	1700
0.2–0.4	D,X	D,X	D,X	D,X
0.5–0.7	D,X,T,S	D,X,T,S,O	D,X,S	D,X,S
1.0–1.5	D,X	D,X,O	D,X	D,X

[a] D = density, X = x-ray diffraction, T = transmission electron microscopy, S = scanning electron microscopy, and O = optical microscopy.

Each experimental batch consisted of approximately 0.5 g Biso-coated UO_2 microspheres (kernel diameter ≈400 μm, overall diameter ≈500 μm before SiC coating) and 13.9 g Biso-coated graphite spheres (overall diameter ≈800 μm). The graphite spheres were added to make the total batch size large enough to coat properly. After coating, these inert spheres were separated from the UO_2 spheres by size and then discarded.

The ratio of hydrogen to MTS in the coating atmosphere typically ranged from 75 to 90. This is well above the minimum H_2/MTS ratio needed to produce dense coatings but was necessary to achieve good fluidization of the bed.

Coating Rates and Batch Characteristics

Coating thicknesses were measured by microradiography. Dividing the SiC thickness by the coating time yields the coating rate. The "inert" graphite spheres were coated at a different rate than were the UO_2 spheres in the same bed. The larger size and lower density of the graphite spheres resulted in their spending more time at the top of the

bed, where coating rates are lower. Since the coatings on the graphite spheres were not used for study, this difference did not present a problem.

Table 2 gives the pertinent data for the 12 experimental coating runs. The ranges of coating rates actually obtained were generally somewhat narrower than the nominal values given in Table 1.

Table 2. Experimental Conditions and Results for SiC Deposition

Run	Temperature (°C)	Coating Run (μm/min)	Density[a] (Mg/m^3)
SC483	1500	0.42	3.208
SC484	1550	0.40	3.212
SC485	1650	0.43	3.218
SC487	1700	0.42	3.197
SC472	1500	0.70	3.190
SC476	1550	0.75	3.207
SC477	1650	0.71	3.203
SC475	1700	0.50	3.195
SC479	1500	1.20	3.156
SC473	1550	1.01	3.195
SC480	1650	0.95	3.207
SC481	1700	1.06	3.206

[a]Standard deviation of coating density by the gradient column method is typically ±0.001 to ±0.008 Mg/m^3.

Characterization Techniques

Transmission Electron Microscopy

Specimens were prepared by vacuum hot-pressing at 640°C and 18 MPa coating fragments dispersed in aluminum powder. Slices were diamond sawed from the resulting cylindrical pellets and ground and lapped until

the slices containing several radially oriented SiC fragments were approximately 20 μm thick. At this stage, the aluminum was usually somewhat thinner than the SiC fragments.

After lapping the aluminum-SiC composite, a 3-mm-diam disk was punched out and thinned by ion milling. Argon was used as the milling gas and ion currents were about 20 μA. Thinning was typically completed in 30 to 50 h.

Specimens were examined in the JEM 100CX* electron microscope at an accelerating voltage of 120 kV. Two modes of operation were employed: selected-area magnification (SAM) and selected-area electron diffraction (SAD). Selected-area magnification (diffraction contrast) produced images of the microstructure at magnifications ranging from 10,000 to 50,000. Conventional bright- and dark-field conditions were used, as well as weak-beam dark-field imaging. Selected-area diffraction was used to measure lattice parameters, identify phases and polytypes, and provide information on twinning and faulting.

X-Ray Diffraction

Coating fragments were mixed with a drop of ethyl alcohol, and the slurry was deposited on a polished single-crystal substrate of silicon. The silicon crystal was cut so that the surface normal was about 7° off the (111) pole and thus provided a low-background substrate for x-ray diffraction analysis. The samples were analyzed in a vertical diffractometer fitted with a diffracted-beam graphite monochromator. Data were collected on paper tapes via a Teletype† printer. The scan speed in 2θ was 0.0021 °/s. The information on the paper tape was subsequently recorded on computer cards, and the x-ray profiles were plotted with a Calcomp plotter. The advantage of this plotting procedure is that the data can be recorded without operator attention, and small peaks can be

*JEOL Ltd., Tokyo, Japan.

†Teletype Corp., Skokie, Ill.

examined at a later time after the sample has been removed from the x-ray unit. This technique has been shown to provide excellent sensitivity and can be used with as little as 1 mg of fragments.

Optical Microscopy

Coating fragments dispersed in aluminum were examined optically before ion milling. Transmitted-light microscopy was used to examine the specimens for large features, such as striations and macroporosity. Polarized light was used to test for optical activity (anisotropy). In addition to examination in the visible range, an infrared imaging tube was used to examine the optical properties of the coatings in the near-infrared region.

Density

The density of a sample of SiC coating fragments is measured by comparison with standards of known density in a density gradient column, according to Procedure MET-CER-TS-18. The entire test specification is included as the Appendix and is briefly summarized below:

1. Coatings are cracked from a number of particles and heated overnight at 800°C in air to oxidize and remove any pyrocarbon.

2. Coating fragments are ultrasonically cleaned in toluene, dried, and ultrasonically wetted with tetrabromoethane.

3. A column is prepared from a mixture of tetrabromoethane and diiodomethane such that the liquid density varies from 3.151 Mg/m^3 at the top to 3.221 Mg/m^3 at the bottom.

4. The coating fragments and density standards are placed in the column and allowed to settle overnight.

5. From the relative position of the coating fragments and standards, the SiC density is calculated.

Scanning Electron Microscopy

Entire SiC-coated particles were examined in the JSM-U3* scanning electron microscope to determine the effect of deposition temperature on surface morphology. As shown in Table 1, for this preliminary study SEM samples were taken from coating runs at the intermediate coating rate for all four temperatures studied. Magnifications were 300, 1000, and 3000.

RESULTS AND DISCUSSION

Transmission Electron Microscopy

To demonstrate the potential of TEM to reveal the fine microstructural features, SiC coatings SC207†, SC472, and SC476, deposited under three different sets of conditions, were examined in detail. In general, growth under vapor deposition conditions produced columnar grains with their major axes oriented radially (i.e., parallel to the growth direction). An example of the columnar grain structure in SC472 is shown in Fig. 3, with the growth direction noted on the micrograph.

The major phase present in all three coatings is fcc β-SiC, determined by both selected-area electron diffraction (SAD) and x-ray diffraction analyses. In addition, small amounts of what appears to be hexagonal α-SiC were detected in SC472. This observation agrees with x-ray results for the same coating, in which several weak α-SiC diffraction peaks were observed.

One SiC grain with some α phase present is shown in Figs. 4 through 6. The bright-field micrograph, Fig. 4, shows a dense network of sharp parallel lines delineating the α phase within the β matrix. Similar micrographs of α and β phases in hot-pressed and sintered SiC have been published by Heuer and coworkers.[5] These thin laths of the α phase produce extensive streaking in the SAD pattern, Fig. 5, in a direction perpendicular to the thin dimension of the laths (which is also the *C*-axis of the α crystal structure). When a dark-field image was formed

---

*JEOL Ltd., Tokyo, Japan.

†Coatings SC207 was an archival sample deposited at 1575°C at a coating rate of 1.36 μm/min.

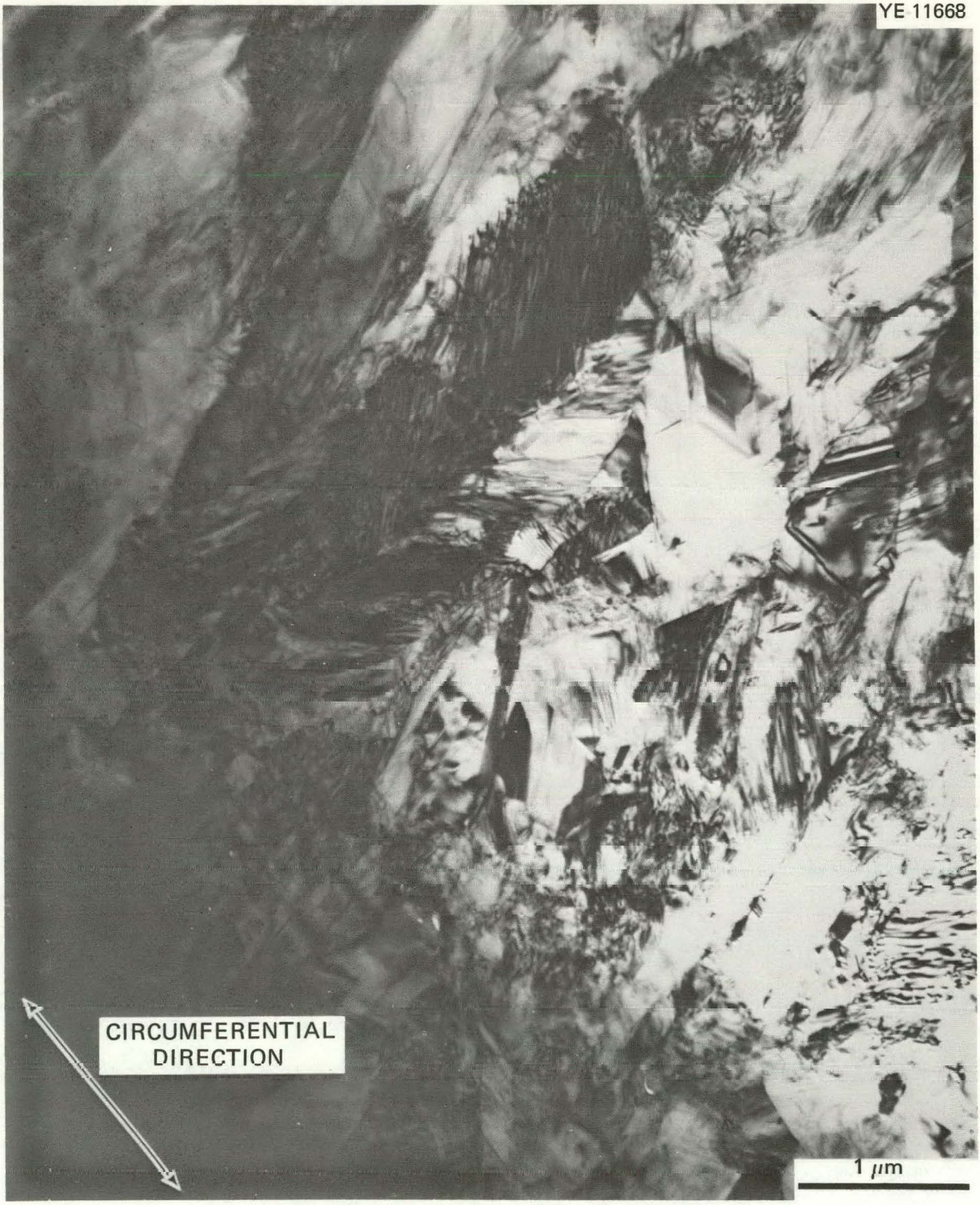

Fig. 3. Columnar Grain Structure in SC472. Coating deposited at 1500°C, 0.70 μm/min. Density = 3.190 Mg/m^3.

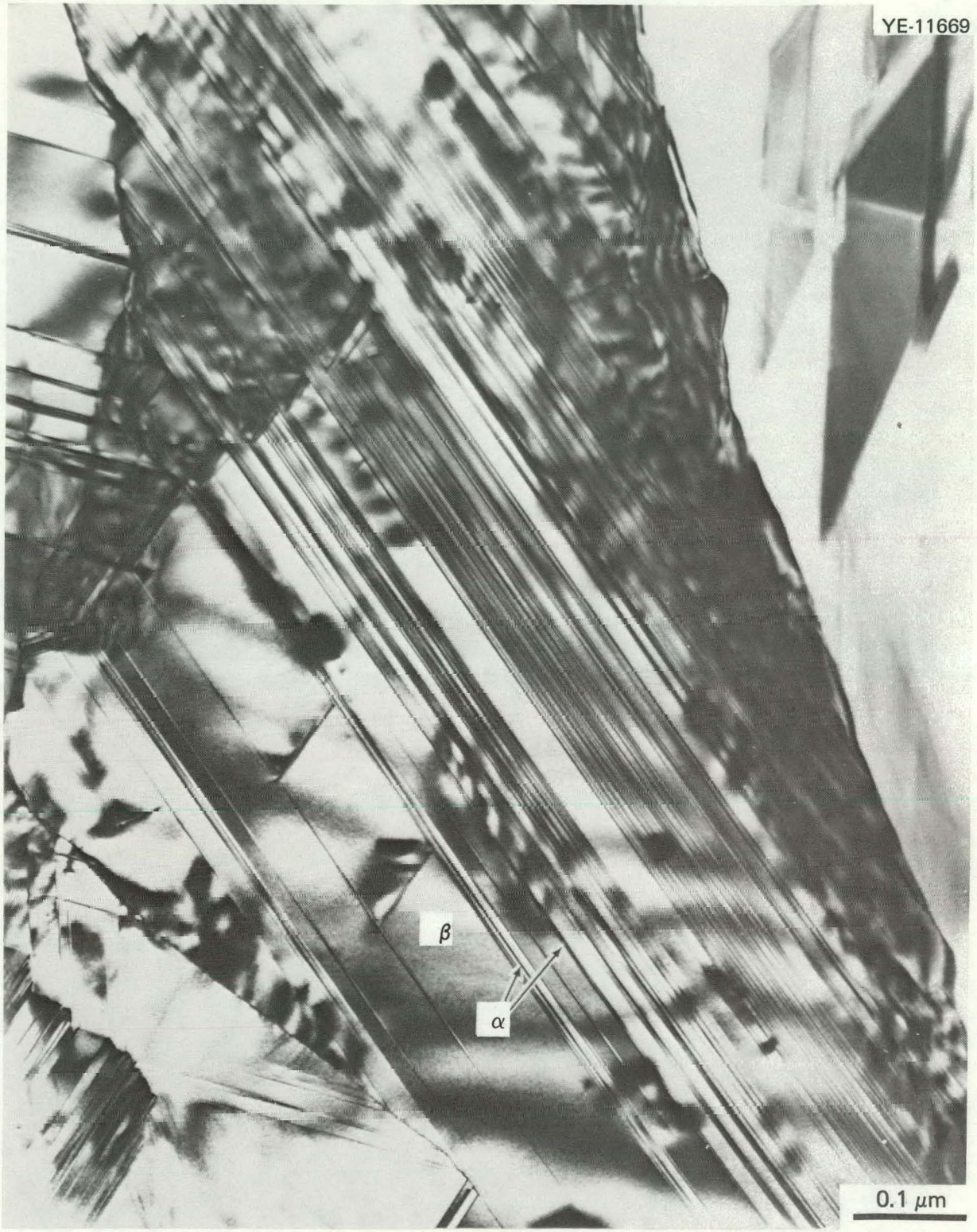

Fig. 4. Bright-Field Micrograph of SC472 Showing α (Hexagonal) and β (Cubic) Phases.

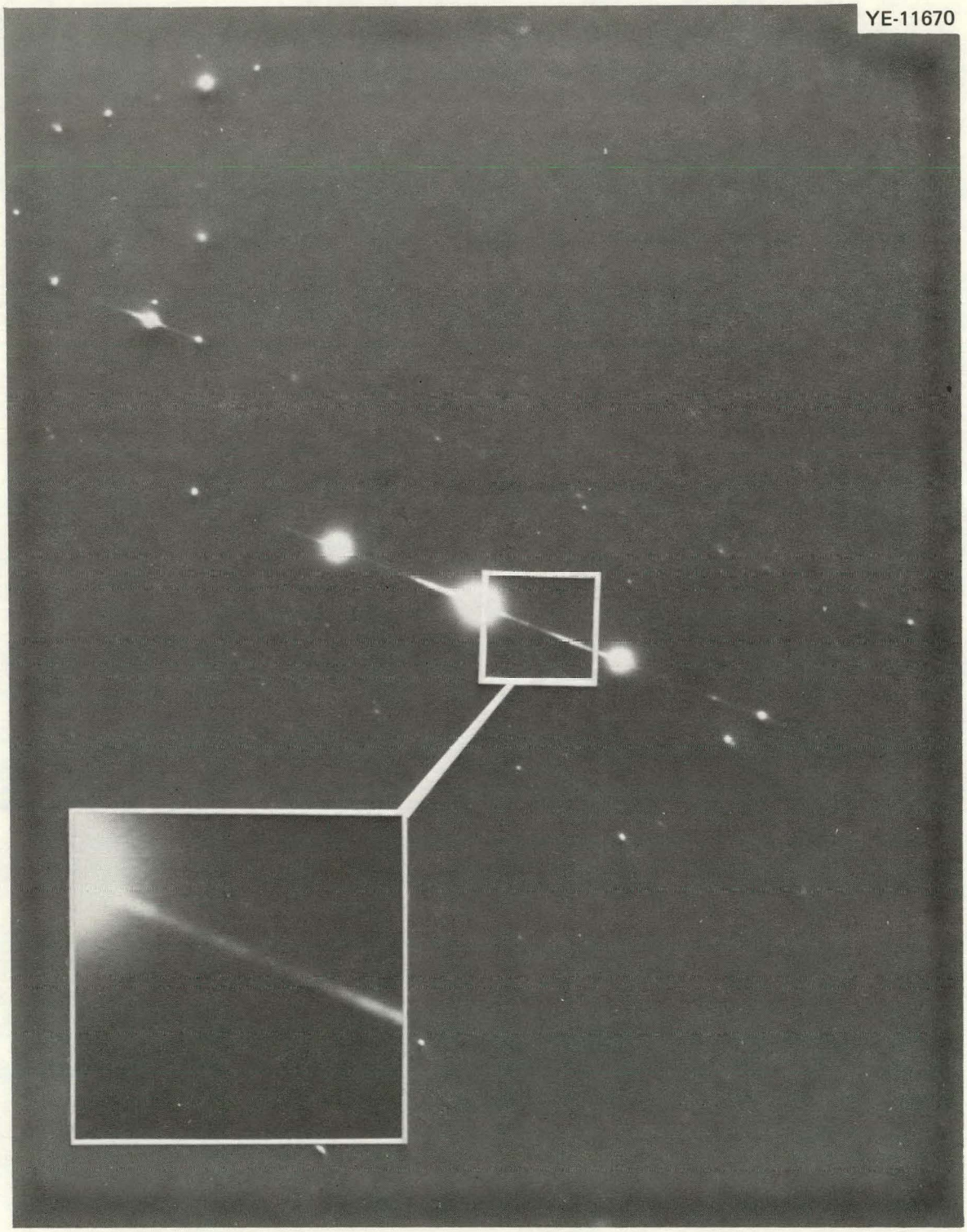

Fig. 5. Electron Diffraction Pattern from the Area of Fig. 4 Containing Both α and β Phases.

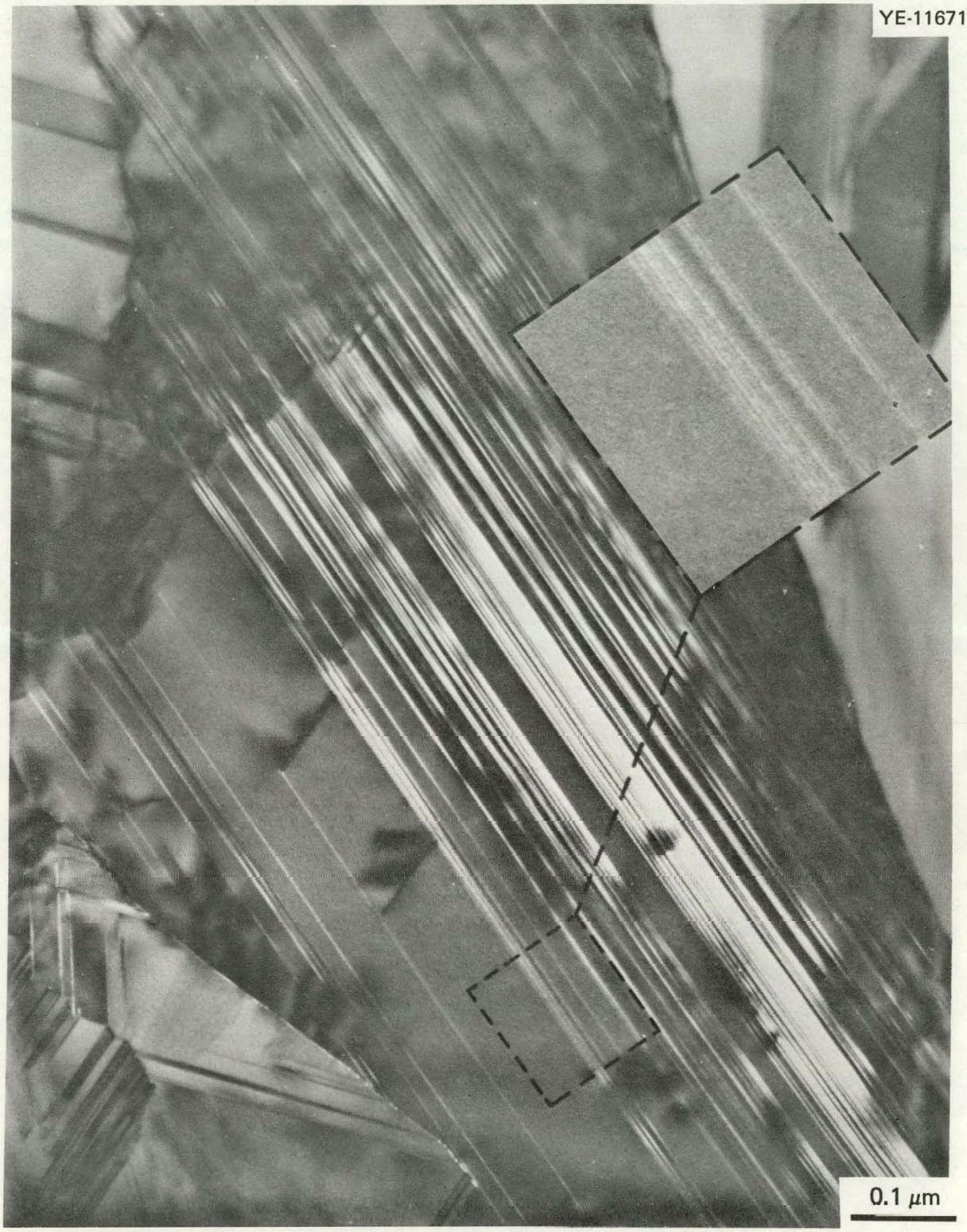

Fig. 6. Dark-Field Micrograph of SC472, Showing α Phase and 1.5-nm Lattice Fringes of the 6H α-Phase Polytype Structure.

by use of a portion of the intensity streak adjacent to the (000) spot, the thin laths were illuminated as shown in Fig. 6. Since the objective aperture was close enough to the (000) spot to intercept some of the transmitted beam, some lattice fringe images were formed of the α phase. The smallest fringes were 1.5 nm apart, indicating that the structure is of the 6H polytype. (For the 6H polytype of α-SiC $c_0 \approx 1.5$ nm.) This particular polytype was also observed by Heuer and coworkers[5] in their material. Fringes with 3 to 4 nm spacings are also present in Fig. 5, so the α material may actually be a mixture of 6H and 15R polytypes. Such mixtures have been observed in reaction-sintered α-SiC by Sato and Shinozaki.[6] Along the streaks in the SAD patterns they found discreet spots of intensity, which could be indexed (by their separation) with the two separate phases. We observed a number of spots along the streaks in Fig. 5 with separations that would be expected for both 6H and 15R polytypes. However, the periodicity was not as regular as it was in those observed by Sato and Shinozaki. Therefore, additional polytypes of α might be present in small amounts in the α regions.

One final observation in the bright-field dark-field pair, Fig. 4 and 6, is that extremely small particles of α also appear to line a grain boundary in the area. An alternate explanation for the structures shown might be related to one-dimensional disorder in β-SiC as described by Sato and Shinozaki[7] in a more recent experiment. Random stacking in the c-direction would, indeed, produce streaking similar to that observed in the present work. However, the lattice images, the presence of small particles in the grain boundary, and the presence of sharp x-ray diffraction peaks matching those expected for α polytypes lend support for interpretation of the data in favor of identification as a true α phase rather than a one-dimensionally disordered β phase.

The defects present in the deposited SiC coatings were extremely complex, as illustrated by the weak-beam dark-field image shown in Fig. 7. Dense networks of stacking faults and/or microtwins are present, as well as complex arrays of lattice dislocations. The relationship of these defects to either the deposition parameters or the coating properties has not yet been determined.

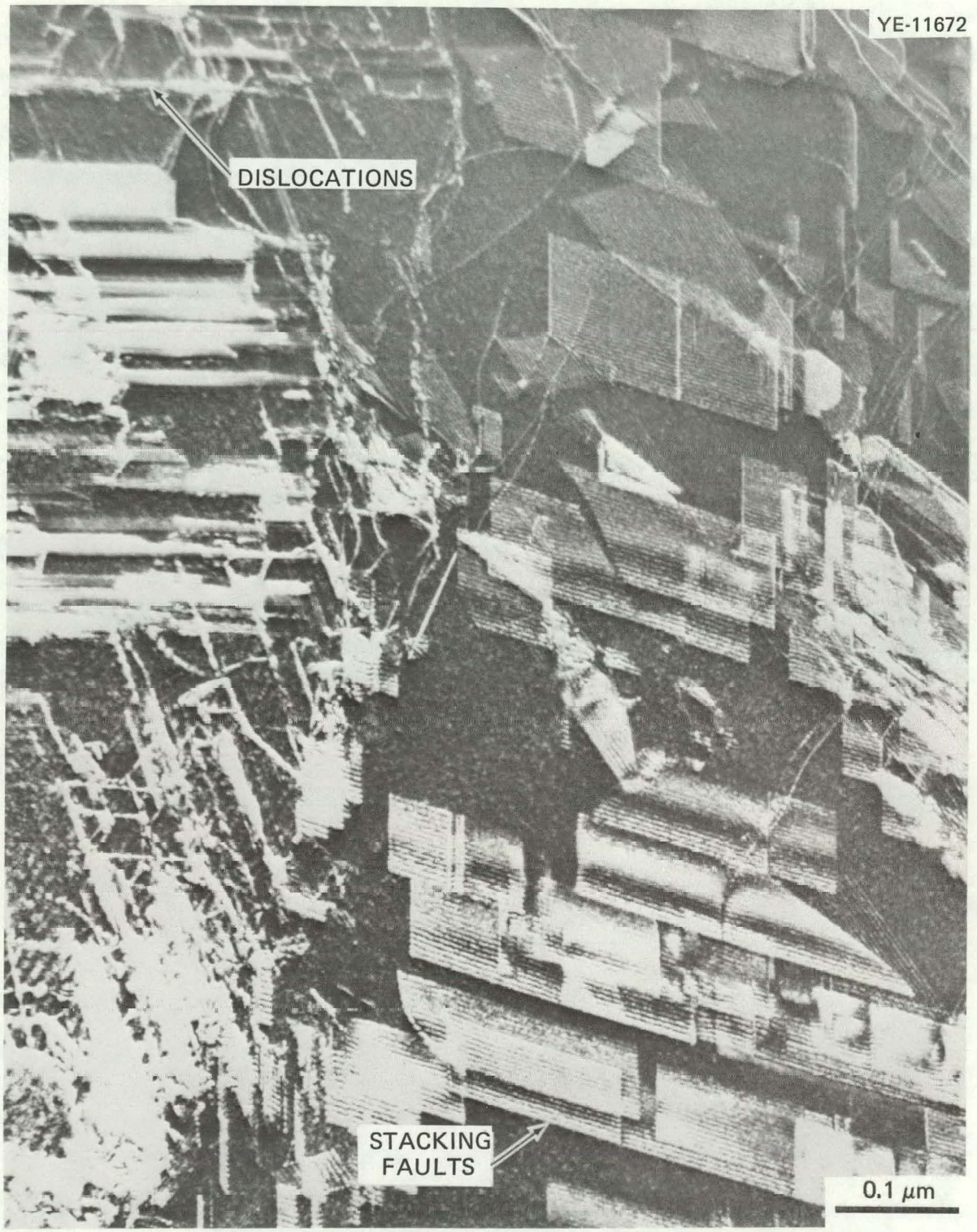

Fig. 7. Defects in SC472, Weak-Beam Dark-Field Image.

Polygonal cavities were present in all three specimens examined and usually lay along grain boundaries. Large strings of cavities, as shown in Fig. 8, were occasionally found and were always oriented along the circumferential direction. In coating SC207, deposited at the relatively high rate of 1.35 μm/min, small cavities (about 5 nm in diameter) were found to lie in rafts on the {111} planes parallel to the stacking faults, as well as on the grain boundaries. Cavities in the SiC coatings are important because they could form paths of high mobility for fission products.

X-Ray Diffraction

The results of all x-ray diffraction analyses are listed in Table 3 and presented graphically in Fig. 9, which allows the effects of deposition temperature and coating rate to be more readily appreciated. The data include specimens deposited in a larger coating furnace by another group.

Table 3. Coating Specimens Examined by X-ray Diffraction

Run	Deposition Temperature (°C)	Coating Rate (μm/min)	Phases
SC207[a]	1575	1.36	α + β
SC483	1500	0.42	β
SC484	1550	0.40	β
SC485	1650	0.43	β
SC487	1700	0.47	β
SC472	1500	0.70	α + β
SC476	1550	0.75	β
SC477	1650	0.71	β
SC475	1700	0.50	β
SC479	1500	1.20	α + β
SC473	1550	1.01	α + β
SC480	1650	0.95	β
SC481	1700	1.06	β
A742[b]	1475	0.15	α + β
A736[b]	1475	0.37	α + β
A508[b]	1475	0.45	α + β
A739	1675	0.37	β

[a] Run SC207 is from earlier work using the same coating furnace.

[b] Runs made in the large (0.13-m) coating furnace.

Fig. 8. Micrograph of SC472, Showing Large Polygonal Cavities.

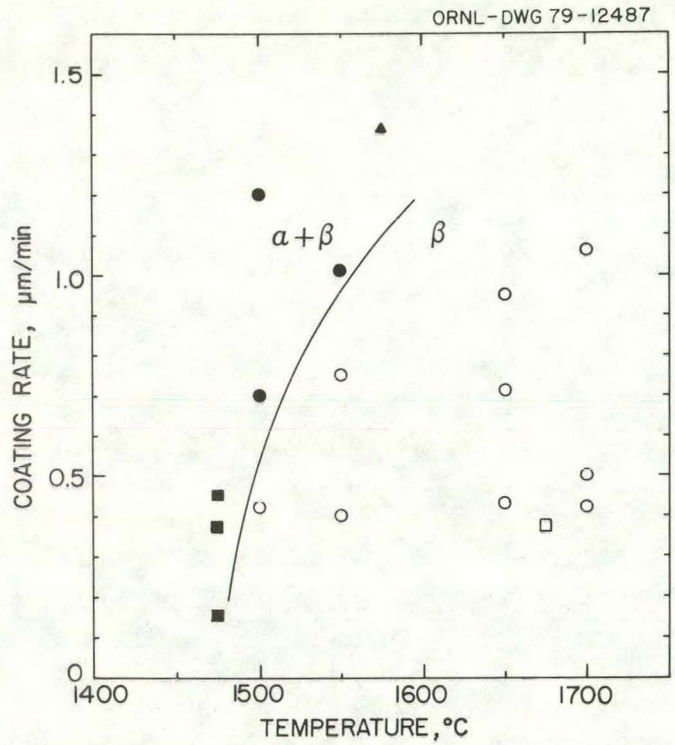

Fig. 9. Phases Present in Chemically Vapor Deposited SiC Coatings as a Function of Deposition Temperature and Coating Rate. Circles indicate coatings made in the small coater, and squares indicate those from the large coater. Triangle point is from an earlier work, small coater. (Solid points indicate coatings that contain some α-SiC, while open points indicate coatings that are 100% β-SiC.)

In one specimen, SC472, the extra diffraction lines have been tentatively indexed as the 15R polytype of α-SiC. Previously, it was assumed that SiC deposited according to the narrow range of parameters used in this study would be 100% β-SiC. Voice and Scott[8] report that very low-temperature deposits (~1200°C) contain as much as 30% of a "disorganized phase," which is not a true α-SiC structure. Price[9] reports that additional diffraction lines are seen in coatings deposited at temperatures below 1500°C. This phase has been identified as disorganized β,[10] disorganized α,[11] type I α,[12] or type 6H α-SiC.[13] In addition to the effect of deposition temperature, Ford and coworkers[11] report a dependence on coating rate. A direct comparison of the present results with those of Ford is impossible because in that work the coating rate was expressed

in terms of mass of SiC per unit time, and this cannot be converted directly to coating thickness per unit time without detailed knowledge of batch and particle sizes.

The present results are interesting in that some α-SiC was apparently formed under conditions that yielded coatings of high density containing no detectable free silicon. The significance of this small amount of what appears to be α-SiC in the coating and its effect on fission-product retention and other properties are not yet known. However, the ease with which extra diffraction peaks can be detected, as demonstrated by this work, may make them useful as an indicator of the quality of the SiC for fission product retention.

Optical Microscopy

As indicated in Table 1, two coating specimens were selected for optical examination. These specimens, SC473 and SC476, were both deposited at 1550°C, at coating rates of 1.01 and 0.75 μm/min, respectively. Thus, one specimen (SC473), contained some α-SiC, while the other was all β-SiC.

Figure 10 shows the optical behavior of SC473, which is typical of both specimens. Figure 10(a) is a bright-field transmitted-light

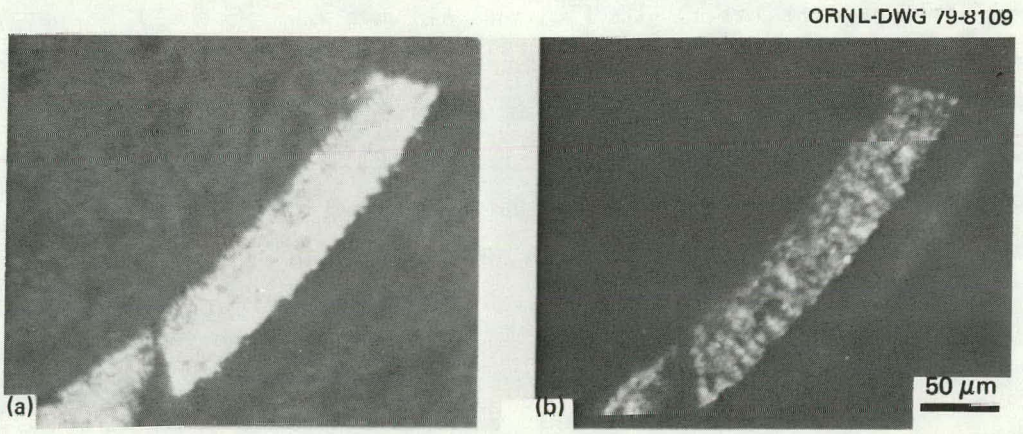

Fig. 10. Transmitted-Light Micrograph of Specimen SC473. (a) Bright field. (b) Crossed Nicols, showing optical activity (anisotropy).

micrograph. The coating fragment appears transparent, surrounded by the opaque aluminum matrix. Figure 10(b) shows the same fragment with plane polarized light with the analyzer oriented perpendicular to the plane of polarization. In this condition, an optically isotropic material would appear black. Thus, the grains that are clearly visible as bright spots are optically anisotropic. This result is unexpected in a cubic material and was observed in both the visible and the infrared regions. It was seen equally well in the specimen that is all cubic β-SiC, and consequently cannot be due to traces of hcp (α) grains alone.

While the cause of this anisotropy is not understood at this time, there are two possible causes:

1. an effect of polytypism that gives rise to optical activity while retaining the "cubic" x-ray diffaction lines,
2. strain-induced birefringence due to grown-in stresses in the coatings.

Further investigations should be conducted to better understand this puzzling phenomenon. If it is due to strain-induced birefingence it may be a key property to look for in production coatings, since residual stresses in the coating may affect irradiation performance.

Density

The results of density measurements in Fig. 11 show a general trend of decreasing density with increasing coating rate. Densities generally reached a maximum at around 1600°C, and all but one of the 12 experimental coatings had densities well above the currently specified minimum density of 3.18 Mg/m^3. Several coatings were sampled from other runs made under similar conditions on kernels that contain simulated fission products. These are indicated on the figure, and the agreement is good.

At high deposition temperatures, the densities of coatings deposited at the highest rate are seen to exceed those of coatings deposited at lower coating rates. This effect has been reported previously.[1] While the cause of this is not yet understood, it could be annealing during the coating process. The particles spend less time at temperature (for a given coating thickness) if the coating rate is high.

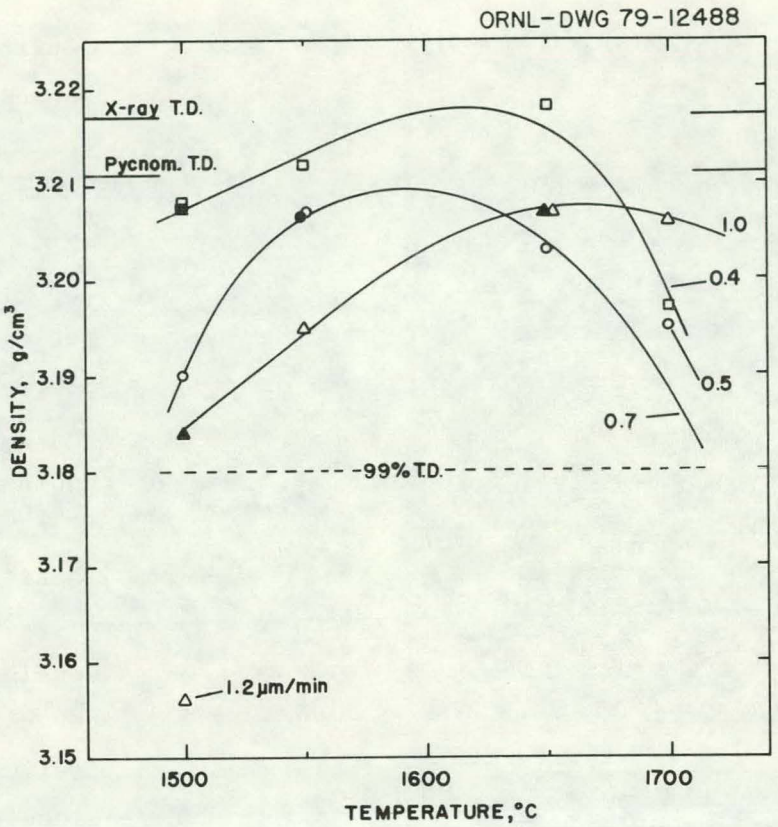

Fig. 11. Densities of SiC Coatings as a Function of Deposition Temperature and Coating Rate. (Coating rates are given in μm/min.) Open points indicate UO_2 kernels, while solid points indicate kernels containing both UO_2 and fission-product elements.

Scanning Electron Microscopy

Examination of the surface morphology of whole coated microspheres revealed the strong effect of deposition temperature. Figure 12 shows the surfaces of coatings deposited at various temperatures at about the same coating rate. The surface features observed can provide information on the crystalline structure of the coating.

The coating deposited at 1500°C, Fig. 12(a), has a botryoidal or globular appearance. Small crystalline facets are evident but not very well developed. The coating deposited at 1550°C, Fig. 12(b), has a good appearance suggestive of a dense, well-developed grain structure. No void spaces are evident. Figure 12(c) shows the coating deposited at 1650°C. This coating also has a dense structure, the individual grains being

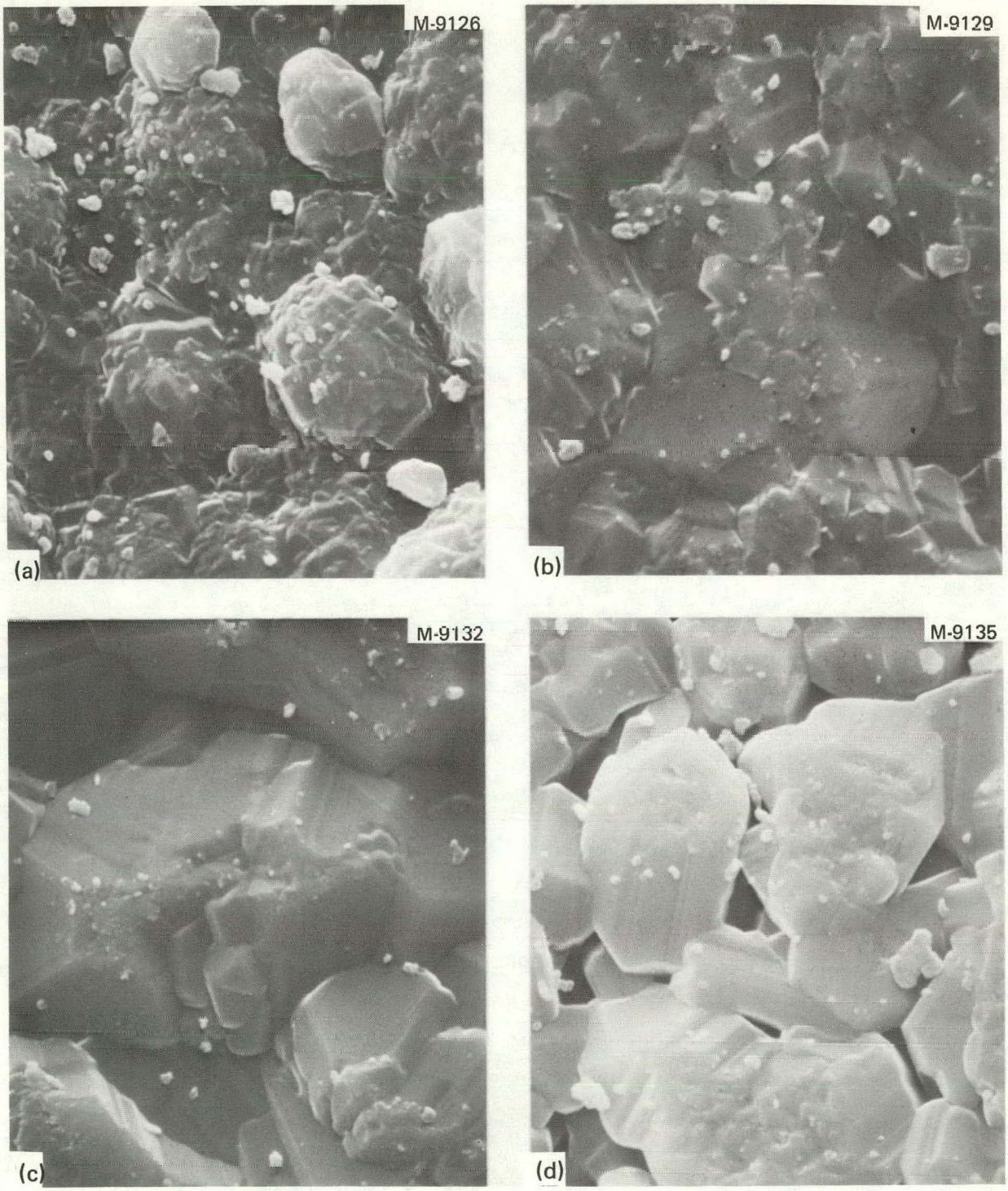

Fig. 12. Scanning Electron Micrographs of SiC Coating Surfaces at 3000×. Coating rates about 0.7 μm/min. Deposition temperatures are: (a) 1500°C, (b) 1550°C, (c) 1650°C, and (d) 1700°C.

somewhat larger than those formed at 1550°C. Some striations are evident on the crystal faces and are probably a result of fluctuations in the growth process. At 1700°C, Fig. 12(d), large individual grains are formed with void spaces between. It should be noted that the density of this coating is not as low as the surface morphology would indicate. Evidently, at this temperature certain favorably oriented grains can grow rapidly outward, while the interstices fill in more slowly.

Not surprisingly, the coatings that show the best surface appearance, Fig. 12(b) and (c), have the highest densities as well. All these observations are in substantial agreement with those reported by Federer.[1] This is particularly encouraging when it is recalled that the batch sizes used in this experimental program were much smaller than those used by Federer. It shows that the coating process was not distorted by the presence of larger graphite spheres used to dilute the particle bed.

CONCLUSIONS

1. The microstructures of chemically vapor-deposited SiC coatings are very complex and must be examined at the submicron level for meaningful characterization.

2. Electron diffraction, lattice imaging, and x-ray diffraction indicate that some coatings contain a second phase, which appears to be one or more polytype forms of α-SiC.

3. The deposition conditions (temperature and coating rate) that give rise to traces of α-SiC in the coating were determined and appear to be independent of coater size and other batch characteristics.

4. Coatings of SiC examined in transmitted polarized light contain numerous optically anisotropic grains. This is unexpected in a cubic material and could be due to residual (grown-in) stresses or polytypism.

5. Density of SiC coatings can be related to deposition temperature and coating rate and is independent of kernel composition. Generally, coating densities reach a maximum at deposition temperatures of approximately 1600°C.

6. The surface morphology of SiC coatings depends very strongly on deposition temperature. The best surface appearance corresponds to deposition temperatures from 1500 to 1650°C, the same range in which coating density reaches a maximum.

ACKNOWLEDGMENTS

The authors would like to thank the following persons and acknowledge their contributions to this work:

J. W. Geer prepared the coatings and separated the samples. W. R. Johnson hot-pressed sample fragments in aluminum. H. Keating prepared transmission electron microscopy specimens and measured densities. W. H. Smith performed the x-ray diffraction measurements.

A. E. Pasto provided UO_2 microspheres. L. A. Harris assisted with the optical measurements. T. J. Henson made scanning electron micrographs. D. P. Stinton provided samples from the large coating furnace.

J M Robbins and T. N. Tiegs reviewed the manuscript, S. Peterson edited the report, and Karen Perry typed and assembled the final version.

REFERENCES

1. J. I. Federer, *Fluidized Bed Deposition and Evaluation of Silicon Carbide Coatings on Microspheres*, ORNL/TM-5152 (January 1977).

2. D. P. Stinton and W. J. Lackey, *Effect of Deposition Conditions on the Properties of Pyrolytic Silicon Carbide Coatings for High-Temperature Gas-Cooled Reactor Fuel Particles*, ORNL/TM-5743 (October 1977).

3. G. Fritz et al.,"Gewinnen Ringförmiger Chlorierter Siliciummethelen-verbindungen (Cyclocarbosilane) aus CH_3SiCl_3, $(CH_3)_2SiCl_2$, und $(CH_3)_3SiCl$," *Z. Anorg. Allg. Chem.* 302: 60–80 (1959).

4. G. Fritz et al., "Die Bildung Chlorierter Silicium-Methylene bei der Pyrolyse der Methylchlorosilane," *Z. Anorg. Allg. Chem.* 322: 46–57 (1963).

5. A. H. Heuer et al., "$\beta \rightarrow \alpha$ Transformation in Polycrystalline SiC: I, Microstructural Aspects," *J. Am. Ceram. Soc.* 61: 406–12 (1978).

6. H. Sato and S. Shinozaki, "Microsyntaxy and Polytypism in SiC," *Mater. Res. Bull.* 9: 679–84 (1974).
7. H. Sato and S. Shinozaki, "One Dimensionally Disordered Structure and Polytypism in SiC," *Mater. Res. Bull.* 10: 257–60 (1975).
8. E. H. Voice and V. C. Scott, "The Formation and Structure of Silicon Carbide Pyrolytically Deposited in A Fluidized Bed of Microspheres," pp. 1–30 in *Special Ceramics 5, Proc. 5th Symp. Special Ceramics,* British Ceramic Society, Stoke-on-Trent, England, 1972.
9. R. J. Price, "Properties of Silicon Carbide for Nuclear Fuel Particle Coatings," *Nucl. Technol.* 35: 320–36 (1977).
10. E. H. Voice and D. N. Lamb, *The Deposition and Structure of Pyrolytic* Silicon Carbide, Dragon Project Report DP-677 (October 1969).
11. L. H. Ford et al., "Fluidized-Bed Pyrolytic Silicon Carbide," pp. 49–69 in *Special Ceramics 5, Proc. 5th Symp. Special Ceramics,* British Ceramic Society, Stoke-on-Trent, England, 1972.
12. T. D. Gulden, "Deposition and Microstructure of Vapor Deposited Silicon Carbide," *J. Am. Ceram. Soc.* 51: 424–27 (1968).
13. B. Hudson et al., *A Transmission Electron Microscopic Study of Pyrolytic and Self-Bonded Silicon Carbide,* AERE-R-7116 (1972).

APPENDIX

Procedure for Density Determination

PAGES 29 to 30

WERE INTENTIONALLY

LEFT BLANK

Procedure for Density Determination

Ceramics Development
Metals and Ceramics Division
OAK RIDGE NATIONAL LABORATORY

Procedure No. MET-CER-TS-18
Revision No. 2
Date August 18, 1975
Page 1 of 2

TEST SPECIFICATION

TITLE: Determination of Particle Coating Density by Gradient Column

PREPARED BY: R. L. Beatty and J. I. Federer — Aug. 19, 1975 (date)

APPROVED BY: W. P. Eatherly — Aug 19, 1975 (date)

DQAC APPROVAL: R. J. Beaver — Aug 20, 1975 (date)

1. Scope: This specification outlines procedures to be followed for gradient column density determinations including sampling, sample preparation, column preparation, and data reporting for pyrocarbon (PyC) and silicon carbide (SiC) coating fragments removed from microspheres.

2. Request: Request for control analysis shall be submitted on forms MET-CER-D-16 and UCN-1910. Examples of these forms are appended to this procedure.

   The original investigator will indicate on form UCN-1910 any special precautions to be taken with the sample (e.g., enriched-fissile and fertile, SiC and/or pyrocarbon coated, pyrophoric, disposition of samples, etc.)

3. Sampling: All coated particles to be tested are to be selected by riffling in accordance with ASTM Standard E 300-70.

4. Specimen Preparation: Individual coated particles are to be cracked using a device which employs a micrometer head to force each particle against a glass plate while the particle is viewed with a low-power microscope. At least 30 fragments of each type of coating layer must be obtained. Care is to be taken that each PyC fragment contains only one layer. Duplicate samples of each layer are to be collected, bottled, and labeled. Fragments from SiC layers will be heated to 1000 ± 25°C for 3 ± 1/2 hr in air while contained in a platinum or alumina (Al_2O_3) crucible to burn away adhering PyC. Any residue from this treatment shall be removed by ultrasonic cleaning for 5 min or until all residue is removed. During ultrasonic cleaning the SiC fragments will be contained in a vial or test tube along with a volatile liquid such as benzene to conduct the ultrasonic vibrations. The completeness of cleaning will be assessed by viewing the fragments at a magnification of at least 30×.

5. Column Preparation: The density gradient column shall be prepared by any established technique which produces either a constant gradient or a curve whose first derivative does not change sign within the working range. Any pair of completely miscible liquids having respective densities suitably above and below the required working range may be used. A set (specified number) of density

standards shall be placed in the column either before or after filling. After the column is established, the standards shall be counted to ensure that the complete set is loaded. Standards shall be positioned in the column working range at increments ≤ 0.10 g/cm^3 for carbon and ≤ 0.025 g/cm^3 for SiC. Each standard must be a spheroid with aspect ratio ≤ 1.5 and density calibrated to ± 0.001 g/cm^3. The column gradient shall be such that the gradient across the vertical dimension of each floating standard is ≤ 0.003 g/cm^3.

6. Specimen Loading: The coating fragments will be placed in a chamber which will be evacuated to a pressure ≤ 1 torr for at least 5 min. The sample will then be submerged, without allowing exposure to other atmospheres, in a mixture of the gradient column liquids having a density 0.10 g/cm^3 less than the estimated density of the fragments. After readmitting atmosphere to the chamber, the liquid will be decanted and the wetted fragments placed in the gradient column. A cap (rubber stopper or other device) shall be placed on the column after all desired materials are loaded.

   An acceptable alternative method of loading SiC fragments involves ultrasonic wetting. The fragments are placed in a small vial or test tube along with a few cc of liquid drawn from the top of the gradient density column. The container is placed in an ultrasonic bath for about 30 sec to promote wetting of the fragments. Then, the liquid containing the wetted fragments is drawn into a medicine dropper and discharged into the top of the gradient density column.

7. Data Recording: After checking to assure no specimen-standard interactions, positions of all standards and specimens shall be observed after a 2-hr settling period for PyC and after 6 hr for SiC fragments. Position measurements shall be made on a scale with smallest division (not interpolation) corresponding to a column density increment ≤ 0.001 g/cm^3. Readings shall be taken on all objects, including standards and fragments, consecutively from top to bottom of column to minimize relative shifts due to temperature fluctuations. Data including the density of each fragment and the density mean and standard deviation for all fragments of each batch shall be reported on form MET-CER-D-35. In addition, the complete column density data with positions shown for all standards will be reported.

ORNL/TM-6940
Distribution
Category UC-77

INTERNAL DISTRIBUTION

1–2. Central Research Library
3. Document Reference Section
4–5. Laboratory Records Department
6. Laboratory Records, ORNL RC
7. ORNL Patent Section
8. P. Angelini
9. D. E. Bartine
10. R. L. Beatty
11. E. E. Bloom
12. D. N. Braski
13. A. J. Caputo
14. J. A. Carpenter, Jr.
15. O. B. Cavin
16. W. P. Eartherly
17. J. I. Federer
18–20. M. R. Hill
21. F. J. Homan
22. D. R. Johnson
23. M. J. Kania
24–33. P. R. Kasten
34. W. J. Lackey
35–44. R. J. Lauf
45. F. L. Layton
46. K. H. Liu
47. E. L. Long, Jr.
48. A. L. Lotts
49. J. E. Mack
50. A. E. Pasto
51. R. L. Pearson
52. J M Robbins
53. J. E. Selle
54. J. O. Stiegler
55. D. P. Stinton
56–60. V. J. Tennery
61. S. M. Tiegs
62. T. N. Tiegs
63. C. S. Yust
64. R. W. Balluffi (Consultant)
65. A. L. Bement, Jr. (Consultant)
66. W. R. Hibbard, Jr. (Consultant)
67. E. H. Kottcamp, Jr. (Consultant)
68. M. J. Mayfield (Consultant)
69. J. T. Stringer (Consultant)

EXTERNAL DISTRIBUTION

70. Hanford Engineering Development Laboratory, P.O. Box 1970, Richland, WA 99352

M. J. Carlson

71. Pacific Northwest Laboratory, P.O. Box 999, Richland, WA 99352

S. Goldsmith

72–74. DOE Division of Nuclear Power Development, Washington, DC 20545

A. J. Pressesky, Acting Director
W. W. Ballard, Nuclear Fuel Cycle Program Branch

75. DOE Office of Nuclear Energy Program, Washington, DC 20545

R. L. Ferguson, Director

76. DOE San Francisco Operations Office, 1333 Broadway, Wells Fargo Building, Oakland, CA 94612

Manager

77–78. DOE Oak Ridge Operations Office, P.O. Box E, Oak Ridge, TN 37830

Assistant Manager, Energy Research and Development
S. W. Ahrends

79–254. DOE Technical Information Center, P.O. Box 62, Oak Ridge, TN 37830

For distribution as shown in TID-4500 Distribution Category, UC-77 (Gas-Cooled Reactor Technology).

☆U.S. GOVERNMENT PRINTING OFFICE: 1979-640-079-154